



Thermo-kinetic investigation of the multi-step pyrolysis of smoked cigarette butts towards its energy recovery potential

José Luiz Francisco Alves¹ · Jean Constantino Gomes da Silva¹ · Guilherme Davi Mumbach¹ · Valdemar Francisco da Silva Filho¹ · Michele Di Domenico² · Rennio Felix de Sena³ · Ariovaldo Bolzan¹ · Ricardo Antonio Francisco Machado¹ · Cintia Marangoni¹

Received: 23 July 2020 / Revised: 27 September 2020 / Accepted: 9 October 2020 / Published online: 16 October 2020

© Springer-Verlag GmbH Germany, part of Springer Nature 2020

Abstract

The present study attempts to explore the energy potential of smoked cigarette butts (SCB) through pyrolysis. For the first time, the pyrolysis characteristics, including the kinetic triplet and the thermodynamic parameters, were investigated using non-isothermal thermogravimetry. Firstly, three pseudo-components were successfully deconvoluted from the multiple-step pyrolysis of SCB using the asymmetrical Fraser-Suzuki function, which corresponds to the devolatilization reactions of retained organic volatile components (PS-1), unburned tobacco (PS-2), and cellulose acetate fibers (PS-3). Posteriorly, the isoconversional methods of Friedman, Flynn-Wall-Ozawa, Kissinger-Akahira-Sunose, and Starink were used to obtain the activation energy values, which were lower for PS-1 (from 101.87 to 108.77 kJ mol⁻¹). The frequency factor values for SCB pyrolysis determined by the compensation effect method were 1.77 × 10¹² min⁻¹ for PS-1, 9.44 × 10¹⁶ min⁻¹ for PS-2, and 9.62 × 10²⁰ min⁻¹ for PS-3. According to the master plot method, the three pseudo-components followed *n*th-order reaction models. An acceptable correspondence was observed between experimental and reconstructed pyrolysis behavior, proving the representativity and reliability of the obtained kinetic triplets. Both positive values of ΔH and ΔG suggest that the pyrolytic conversion of smoked cigarette butts into biofuels can be considered as a non-spontaneous conversion. These pyrolysis-related findings from SCB can be used to offer a good opportunity for its valorization as an energy commodity instead of a neglected solid residue.

Keywords Smoked cigarette butts · Pyrolysis kinetics · Deconvolution process · Thermodynamics analysis · Energy recovery

1 Introduction

Currently, the unsustainable consumption of fossil fuels worldwide has encouraged research into the use of waste-to-energy processes. Recovering useful energy from solid wastes

using thermochemical conversion is regarded as a feasible strategy for both waste management and energy production [1, 2]. In Brazil, about 27.9 million people are smokers, consuming 110 billion cigarettes per year [3]. In this context, about 44 thousand tons of smoked cigarette butts (one cigarette butt has an average weight of 0.4 g [4]) are generated as garbage annually in Brazil, consequently, causing several environmental problems due to their toxic and hazardous characteristics [4–7]. The smoked cigarette butts consist mostly of cellulose acetate fibers, and small fractions of harmful substances (such as tar and nicotine), unburned tobacco, ash, and paper [4, 8], which results in a high degree of carbon atoms in its composition [7]. The majority fraction, composed by cellulose acetate, is non-biodegradable [8, 9]; thus, cigarette butts may not be decomposed in a landfill. Public concern over substantial pollution caused by smoked cigarette butts has demanded the search for new recycling routes, which can convert smoked cigarette butts into valuable products and reduce the environmental problems due to their inadequate

José Luiz Francisco Alves and Jean Constantino Gomes da Silva contributed equally to this work and share senior authorship.

✉ José Luiz Francisco Alves
zeluiz_alves@hotmail.com

¹ Graduate Program in Chemical Engineering, Department of Chemical Engineering and Food Engineering, Federal University of Santa Catarina, Florianópolis, Santa Catarina 88040-900, Brazil

² Department of Engineering, Federal University of Technology–Paraná (UTFPR), Francisco Beltrão, Paraná 85601-970, Brazil

³ Laboratory of Activated Carbon, Department of Chemical Engineering, Federal University of Paraíba, João Pessoa, Paraíba 58033-455, Brazil

management. These characteristics indicate that smoked cigarette butts can potentially be used as carbonaceous raw material for energy production. Smoked cigarette butt's disposal often involves inefficient landfilling and incineration; however, they are being discouraged since are not environmentally friendly, sustainable, and feasible disposal options [8]. Alternatively, the predominant effort considers the recycling of smoked cigarette butts based on the production of adsorbent materials for several applications [3, 5, 7, 9]; however, the smoked cigarette butts are still considered solid waste after their use in the form of absorbent materials (becoming saturated), generating secondary pollution, and requiring expensive forms of treatment [8]. In this context, the pyrolysis process appears as an environmentally friendly disposal way for smoked cigarette butts, which provides an opportunity of converting smoked cigarette butts into useful biofuels [8].

Pyrolysis is a promising possibility towards a safe circular economy, as it can handle harmful substances and provides an opportunity of valorization by converting carbon-based materials into energy carriers such as biochar, bio-oil, and pyrolytic syngas [10–12]. There are several benefits of using pyrolysis as a disposal way for solid waste when compared to the landfilling and incineration. For instance, when compared to combustion (or incineration), pyrolysis has a lower process temperature and lower emissions of air pollutants, as well as zero waste generation and more flexible and compact equipment at plant scale [2, 13]. Smoked cigarette butts waste that contains cellulose acetate filters saturated with toxic compounds can be classified as municipal and hazardous waste [4], which requires a long period to decompose in the environment, but that also presents great polluting potential, making unfeasible the use of landfills. In addition, the decreasing amount of land available for solid waste disposal and high maintenance costs have constrained the choice for landfills [14]. For example, disposal in Brazilian landfills is costly, estimated at US\$ 70 per ton [15]. Thus, the pyrolysis of smoked cigarette butts waste seems to be a more adequate disposal way over traditional disposal methods.

Solid residues, as coffee paper cup waste, polyvinylchloride cable sheath, medium density fiberboard, and plastic solid waste, have recently been proposed as feedstocks to the pyrolysis process [1, 16–18]. In this regard, few attempts have been carried out to study the feasibility of smoked cigarette butts in the production of biofuels through pyrolysis [8]. For now, to our knowledge, the present information is insufficient concerning an in-depth understanding of the kinetic and thermodynamic parameters of the pyrolysis of smoked cigarette butts. This detailed knowledge is fundamental to achieving efficient and competitive waste-to-biofuel conversion [16, 17, 19].

Thermogravimetric analysis (TGA) is a useful technique to investigate the solid-state pyrolysis patterns in the form of kinetic curves (conversion rate as a function of temperature

or time) under an oxygen-free atmosphere [20–23]. With the combined use of non-isothermal TGA outputs and mathematical methods, thermal behavior, reaction kinetics, and heat transfer data can be identified and investigated and, together with thermodynamic parameters, they can help to provide a reliable description of the entire pyrolysis process [24–27]. The kinetic triplet, i.e., the apparent activation energy (E_a), the frequency factor (A), and the reaction model ($f(\alpha)$), can be determined by TGA measurements associated to numerical kinetic approximations, which has practical importance to advance in large-scale reactor design [23, 28]. The fundamental concepts of the energy barrier, the frequency of vibrations of the activated complex, and the reaction mechanism have equal significance [29]. The isoconversional methods of Friedman (FR), Flynn-Wall-Ozawa (FWO), Kissinger-Akahira-Sunose (KAS), and Starink (STK) express the values of E_a with the conversion, which can be estimated without the assumption of the reaction model and frequency factor [21–23, 29]. The compensation effect and the master plot methods have been frequently applied to obtain the A and $f(\alpha)$ parameters, respectively and these methods are enabled to attend this study due to their recognized accuracy. Thermodynamic favorability and energy requirements of the pyrolysis process can be evaluated by calculating the thermodynamic parameters such as the enthalpy change (ΔH), Gibb's free energy change (ΔG), and the entropy change (ΔS) by the Eyring Theory [1, 17, 18].

Usually, pyrolysis of solid residues tends to be a complex process since it involves several physical and chemical pathways with the overlapping of numerous reactions [1]. The use of deconvolution has been successfully adopted as a reliable pathway to distinguish and analyze individual processes in a complex pyrolysis reaction [1, 23, 30]. Thus, the kinetic triplet estimated by the sum of the several individual analysis can be useful for the reconstruction of the entire experimental pyrolysis behavior with high accuracy [1, 23]. A reliable description of the entire pyrolysis process, in terms of kinetics and thermodynamic aspects, is essential for the design and scale-up of an effective reactor [26, 27]. In this context, a significant part of the published kinetic studies does not provide sufficiently reliable information on kinetics and thermodynamic parameters since the complex reactions are often interpreted as single-step kinetics, i.e., by a single kinetic triplet. In addition, the validation of the estimated kinetic data is frequently omitted in kinetics investigations, although the ICTAC Kinetics Committee recommends that to ensure data reliability [29]. Although the pyrolysis of smoked cigarette butts has been used for the production of ester-rich bio-oil [8], no research has been done on the pyrolysis characteristics of smoked cigarette butts by exploring its kinetic triplet and thermodynamic parameters, which motivates this study.

The current study represents the first attempt at exploring the pyrolysis kinetics and the physicochemical properties of smoked cigarette butts in order to allow an

evaluation of the energy potential of this solid residue. Firstly, the physicochemical characterization was performed to identify the capacity of the smoked cigarette butts to be used as a feedstock for pyrolysis. The asymmetrical Fraser-Suzuki function was used to deconvolute the overall differential curves into several pseudo-components, while the apparent activation energy was determined, in a second step, using four isoconversional methods (FR, FWO, KAS, and STK). The compensation effect and the master plot methods were adopted for each separate pseudo-component to find the frequency factor and possible pyrolysis reaction models, respectively. The adequacy of the resulting kinetic triplets was tested by the reconstruction of the experimental weight-loss curves. Thermodynamic parameters were also estimated using the Eyring Theory to characterize the conversion of smoked cigarette butts to biofuels. Findings from this study on the smoked cigarette butts subjected to pyrolysis will be critical to transforming this solid waste into a potential energy feedstock on a sustainable basis.

2 Materials and methods

2.1 Collection and preparation of smoked cigarette butts

The smoked cigarette butts (SCB) were collected from the Reitor João David Ferreira Lima University Campus (Federal University of Santa Catarina, Florianópolis) in December 2019. The smoked cigarette butts were ground using a cutting mill (Solab, SL-31, Piracicaba, Brazil) and sieved using a mechanical sieve shaker (Bertel, series 1.0, São Paulo, Brazil) to obtain particles of < 250 μm in size (60 mesh). The powdered sample was stored in a sealed polyethylene bag for later use. Proximate analysis, ultimate analysis, and heating values were carried out to characterize the SCB sample. All the experiments were repeated at least twice, and the characterization results were expressed in terms of averages.

2.2 Physicochemical analyses

On an as-received basis, the percentage by weight (wt%) of moisture (MO), volatile matter (VM), and inorganic material (ASH) in SBC was determined by a thermogravimetric analyzer model TGA-Q50 (TA Instruments, New Castle, USA) following the standard method ASTM E1131-08 [31]. The percentage by weight of fixed carbon (FC) was estimated by difference on an as-received basis, as follows:

$$FC(\text{wt}\%) = 100 \text{ wt}\% - \text{MO}(\text{wt}\%) - \text{VM}(\text{wt}\%) - \text{ASH}(\text{wt}\%) \quad (1)$$

The ultimate analysis is a procedure used to quantify the percentage by weight of carbon, hydrogen, nitrogen, sulfur, and oxygen in an organic compound. In this work, the standard protocol ASTM D5373-08 [32] was used to determine carbon, hydrogen, and nitrogen in an Elemental Analyzer 2400 CHN Perkin-Elmer Series II, while the protocol ASTM D4239-14 [21] was used to determine the sulfur in an ICP-OES Analyzer Spectro Arcos. The oxygen content was determined by the difference in dry weight basis, according to Eq. 2.

$$O(\text{wt}\%) = 100 \text{ wt}\% - C(\text{wt}\%) - H(\text{wt}\%) - N(\text{wt}\%) - S(\text{wt}\%) - \text{ASH}(\text{wt}\%) \quad (2)$$

The Channiwala and Parikh correlation was used to estimate the higher heating value (HHV) on a dry weight basis, according to Eq. 3 [33].

$$\text{HHV}(\text{MJ kg}^{-1}) = 0.3491 \cdot C(\text{wt}\%) + 1.1783 \cdot H(\text{wt}\%) + 0.1005 \cdot S(\text{wt}\%) - 0.1034 \cdot O(\text{wt}\%) - 0.0151 \cdot N(\text{wt}\%) - 0.0211 \cdot \text{ASH}(\text{wt}\%) \quad (3)$$

The lower heating value (LHV), on a dry weight basis, was calculated using an empirical correlation (Eq. 4), which deducts the value of the latent heat of vaporization of water from HHV [34].

$$\text{LHV}(\text{MJ kg}^{-1}) = \text{HHV}(\text{MJ kg}^{-1}) - 0.2183 \cdot H(\text{wt}\%) \quad (4)$$

2.3 Thermogravimetric analysis

Thermogravimetric experiments were performed using a thermogravimetric analyzer model TGA-Q50 (TA Instruments, New Castle, USA) under an oxygen-free atmosphere for pyrolysis. A sample mass of 10 mg was placed into a standard platinum crucible and heated from room temperature to 800 K under controlled high-purity nitrogen (N₂, 99.999%), with a gas flow rate of 50 mL min⁻¹. This procedure was performed for the non-isothermal condition with heating rates of 5, 10, 20, and 30 K min⁻¹. Slow heating rates (≤ 30 K min) and small particle size (< 250 μm) were applied to reduce heat and mass transfer restrictions, as reported by Van de Velden et al. [35]. A purge step with a high purity nitrogen atmosphere (99.999%) was performed by 30 min with a gas flow rate of 50 mL min⁻¹ before each thermogravimetric analysis. This first step was necessary to avoid secondary oxidation reactions during heating. A blank TG run (using an empty sample crucible) was used to eliminate systematic errors from each experimental run of pyrolysis. The described procedures were

adopted following the ICTAC Kinetics Committee recommendations [36].

2.4 Kinetic study

The pyrolysis kinetics of a residue is evaluated through a process of converting solids into volatiles, which occurs by a sequence of chemical reactions. The complex structure of the residue is broken into different small structures by the temperature increase; consequently, the process results in a weight loss of solid structure. This behavior can be mathematically expressed by the following equation [29]:

$$\left(\frac{d\alpha}{dt}\right)_{\text{Biomass}} = A_{\text{biomass}} \cdot e^{E_{a\text{Biomass}}/R \cdot T} \cdot f(\alpha)_{\text{Biomass}} \quad (5)$$

where R ($\text{kJ mol}^{-1} \text{K}^{-1}$) represents the gas constant, α , t , and T are the physical parameters of conversion, time (min), and temperature (K), respectively, while the kinetic parameters of A , E_a , and $f(\alpha)$ are the frequency factor (min^{-1}), apparent activation energy (kJ mol^{-1}), and reaction model, respectively. The physical parameters are detected by thermogravimetric analysis, in which the conversion is represented by the relationship between the initial and final mass of the solid, with the mass for each pyrolysis time, or temperature. Equation 5 (kinetic parameters constants) returns a single thermal behavior, i.e., the parameters from Eq. 5 are suitable for solids with just one thermal behavior [23]. The thermogravimetric data report a mass loss of the solid as an overall behavior; thus, Eq. 5 is unsuitable for a complete description of the thermal behavior since different compounds constitute the structure of residue. The deconvolution method can be useful to predict the thermal behavior of every single possible component decomposed during pyrolysis. In addition, the estimation of the kinetic parameters in a kinetic study is commonly performed by non-isothermal programming at different heating rates. In this context, Eq. 5 is transformed into Eq. 6, which describes the sum of each thermal decomposition of the components of pyrolysis.

$$\left(\frac{d\alpha}{dt}\right)_{\text{Biomass}} \equiv \sum_{i=1}^N c_i \cdot \left(\frac{d\alpha}{dt}\right)_i = \frac{1}{\beta} \cdot \sum_{i=1}^N [c_i \cdot A_i \cdot e^{E_{ai}/R \cdot T} \cdot f(\alpha)_i] \quad (6)$$

where β (K min^{-1}) is the heating rate, c is the contributed fraction in conversion, the subscript i represents each possible component during the pyrolysis of the residue, and N is the total of components proposed for the residue.

2.4.1 Determination of pseudo-components by deconvolution

The complex composition of residues results in the overlapping of each component. The description of each component

can be obtained by the deconvolution method, which offers a reliable way to obtain the curves of the pseudo-components for posterior kinetic evaluation [23, 37]. Perejón et al. [38] compared several functions for deconvolution curves and obtained the best results using the Fraser-Suzuki function. Accordingly, the pseudo-component curves in thermogravimetric data in this work were obtained from the Fraser-Suzuki function.

$$\frac{dm}{dT} = \theta \cdot \exp \left\{ -\frac{\ln(2)}{s^2} \cdot \left\{ \ln \left[1 + 2 \cdot s \cdot \left(\frac{T - T_p}{w} \right) \right] \right\}^2 \right\} \quad (7)$$

where θ is the amplitude, T_p is the peak temperature, w is the half-width in the curve, and s is the asymmetry shape parameter ($s \neq 0$). The sum of each curve is represented by the overall thermal behavior, as shown in Eq. 8.

$$\frac{dm}{dT} = \sum \eta_i \cdot \left(\frac{dm}{dT}\right)_i = \sum \frac{\eta_i}{m_0 - m_\infty} \cdot \left(\frac{d\alpha}{dT}\right)_i \equiv \sum c_i \cdot \left(\frac{d\alpha}{dT}\right)_i \quad (8)$$

where η is the contribution of the pseudo-component i in unit of mass, m_0 is the initial mass, m_∞ is the final mass, and the subscript i represents the pseudo-components in SCB waste. The parameters in Eq. 7 are obtained by minimizing the residual sum of squares (RSS).

$$RSS = \sum \left[\left(\frac{dm}{dT}\right)_{\text{exp}} - \left(\frac{dm}{dT}\right)_{\text{dec}} \right]^2 \quad (9)$$

where M is the total number of points used for the deconvolution, $(dm/dT)_{\text{exp}}$ is the experimental values measured, and $(dm/dT)_{\text{dec}}$ represents the values from deconvolution.

2.4.2 Apparent activation energy determination

The apparent activation energy for each pseudo-component can be estimated after data extraction through the deconvolution method. The determination of E_a values is performed using the integral form and differential form of Eq. 6, which are known as isoconversional methods. The differential form is expressed by Eq. 10, while the integral form is expressed by Eq. 11.

$$\ln \left(\frac{d\alpha}{dt}\right)_i = \ln \left(\beta \cdot \frac{d\alpha}{dT} \right)_i = \ln [A_i \cdot f(\alpha)_i] - \frac{E_{ai}}{R \cdot T} \quad (10)$$

$$g(\alpha)_i = \int_0^1 \frac{d\alpha}{f(\alpha)_i} = \frac{A_i}{\beta} \int_{T_0}^T e^{-E_{ai}/RT} dT = \frac{A_i}{\beta} \cdot I(E_{ai}, T) = \frac{A_i \cdot E_{ai}}{R \cdot \beta} \cdot p(x) \quad (11)$$

where $g(\alpha)$ is the integral form of the reaction model, and $p(x)$ represents an approximation for temperature integral equation with $x = E_a/RT$. The subscript “ i ” represents each possible component during the pyrolysis of the SCB sample.

Unlike the differential expression (Friedman method), the estimation of E_a values from Eq. 11 is not reached since the integral expression does not provide an analytical solution. Thus, approximate equations are alternative solutions to provide expressions with acceptable accuracy and also recommended by the ICTAC Kinetics Committee [29]. The most common integral expressions solved by approximated equations are the methods of Flynn-Wall-Ozawa (FWO), Kissinger-Akahira-Sunose (KAS), and Starink (STK) represented by Eq. 12, Eq. 13, and Eq. 14, respectively [21–23].

$$\log \beta = \log \left(\frac{A_i \cdot E_{ai}}{R \cdot g(\alpha)_i} \right) - 2.315 - 0.4567 \cdot \frac{E_{ai}}{R \cdot T} \tag{12}$$

$$\ln \left(\frac{\beta}{T^2} \right) = \ln \left(\frac{A_i \cdot R}{E_{ai} \cdot g(\alpha)_i} \right) - \frac{E_{ai}}{R \cdot T} \tag{13}$$

$$\ln \left(\frac{\beta}{T^{1.92}} \right) = \text{Constant} - 1.0008 \cdot \frac{E_{ai}}{R \cdot T} \tag{14}$$

A linear regression analysis between the left side of Eq. 12, Eq. 13, and Eq. 14, and $1/T$, is used to obtain the E_a values, i.e., $\log \beta$ versus $1/T$ for the FWO method, $\ln(\beta/T^2)$ versus $1/T$ for the KAS method, and $\ln(\beta/T^{1.92})$ versus $1/T$ for STK method.

2.4.3 Frequency factor determination

The isoconversional methods are not suitable for the determination of the frequency factor due to a lack of knowledge of the reaction model expression. In this case, it is necessary to use alternative methods to determine the values of A , although the presence of A in the expression of isoconversional methods. The compensation effect (Eq. 15) is generally used for the estimation of A and has the advantage of offering a simultaneous evaluation of both $\ln A$ and E_a [29]. The use of the compensation effect method for A determination is in accordance with the ICTAC Kinetics Committee recommendations [29].

$$\ln(A)_i = a_i \cdot E_{ai} + b_i \tag{15}$$

$$\ln \left(\frac{g(\alpha)_{ij}}{T^2} \right) = \ln \left[\frac{A_{ij} \cdot R}{\beta \cdot E_{aij}} \cdot \left(1 - 2 \cdot \frac{R \cdot T}{E_{aij}} \right) \right] - \frac{E_{aij}}{R \cdot T} \tag{16}$$

where a and b are the compensation parameters, and the terms i and j are the residue component and the reaction model, respectively. The method consists of obtaining the compensation parameters from a model-fitting, such as Coats-Redfern method (Eq. 16), at a single heating rate and several reaction models found in the literature, as initial step [39]. After, the plotting provides a straight line, where a is obtained from the slope and b is obtained from the y -intercept. Finally, the values of A are estimated using the compensation

parameters and E_a values previously determined by an isoconversional method.

2.4.4 Reaction model determination

The master plot is often used for the determination of the reaction model in a pyrolysis process [1, 34]. This method is a well-established mathematical procedure, which is based on the comparison between the curves plotted as $g(\alpha)/g(0.5)$ versus α for theoretical and experimental data. The theoretical curves are plotted for several reaction models found in the literature [1, 40], while the experimental curves are obtained from the ratio between the temperature integral equations for each conversion point and the conversion when the reaction reaches 50% (Eq. 17).

$$\frac{g(\alpha)_i}{g(0.5)_i} = \frac{p(x)_i}{p(x_{0.5})_i} \tag{17}$$

Equation 17 indicates that the ratio of the integral function can be associated with the ratio of the integral approximation and the overlapping of Eq. 17 in theoretical curves, providing information about the reaction model.

2.4.5 Reconstruction of the curves using kinetic triplet

The reconstruction of the thermal behavior for each heating rate (5, 10, 20, and 30 K min⁻¹) was performed using the kinetic triplet (determined by isoconversional methods, compensation effect, and master plot) in Eq. 6. Subsequently, the new expression was solved using the numerical method of Runge-Kutta 4th-order, from which are obtained curves in terms of $d\alpha/dt$ versus T . Each experimental condition was overlapped with its respective reconstructed curve to compare both curves and to confirm the obtained kinetic triplet. The curves were mathematically compared using the coefficient of determination (R^2), quality of fit (QOF), residual (y), and mean residual (My), as shown in Eq. 18, Eq. 19, Eq. 20, and Eq. 21, respectively.

$$R^2 = 1 - \frac{\sum \left[\left(\frac{d\alpha}{dt} \right)_{\text{exp}} - \left(\frac{d\alpha}{dt} \right)_{\text{rec}} \right]^2}{\sum \left[\left(\frac{d\alpha}{dt} \right)_{\text{exp}} - \left(\frac{d\alpha}{dt} \right)_{\text{av}} \right]^2} \tag{18}$$

$$QOF(\%) = \left(1 - \frac{\sqrt{\sum \left[\left(\frac{d\alpha}{dt} \right)_{\text{exp}} - \left(\frac{d\alpha}{dt} \right)_{\text{rec}} \right]^2 / N}}{\left[\left(\frac{d\alpha}{dt} \right)_{\text{exp}} \right]_{\text{max}}} \right) \cdot 100 \tag{19}$$

$$y = \left(\frac{d\alpha}{dt} \right)_{\text{exp}} - \left(\frac{d\alpha}{dt} \right)_{\text{rec}} \tag{20}$$

$$My = \frac{\sum \left[\left(\frac{d\alpha}{dt} \right)_{\text{exp}} - \left(\frac{d\alpha}{dt} \right)_{\text{rec}} \right]}{N} \tag{21}$$

where $(d\alpha/dt)_{\text{exp}}$ represents the experimental values of $d\alpha/dt$, $[(d\alpha/dt)_{\text{exp}}]_{\text{max}}$ represents the maximum conversion rate within the experimental values of $d\alpha/dt$, $(d\alpha/dt)_{\text{av}}$ is the average of experimental values of $d\alpha/dt$, $(d\alpha/dt)_{\text{rec}}$ represents the values of $d\alpha/dt$ calculated by the numerical method of Runge-Kutta 4th-order, and N is the number of experimental points used.

2.5 Estimation of thermodynamic parameters

The thermodynamic parameters in pyrolysis process provide valuable information about energy balances. The thermodynamic parameters, i.e., the change of enthalpy (ΔH), change of Gibbs free energy (ΔG), and change of entropy (ΔS), were determined using the activated complex theory (Eyring Theory) [41–43], as follows:

$$\Delta G = E_a + R \cdot T_m \cdot \ln \left(\frac{k_B \cdot T_m}{h \cdot A} \right) \quad (22)$$

$$\Delta H = E_a - R \cdot T \quad (23)$$

$$\Delta S = \frac{\Delta H - \Delta G}{T_m} \quad (24)$$

where k_B is the Boltzmann constant ($1.381 \times 10^{-23} \text{ J K}^{-1}$), h is the Plank constant ($6.626 \times 10^{-34} \text{ J s}^{-1}$), and T_m is the maximum temperature peak observed from the differential thermogravimetric (DTG) curve.

3 Results and discussion

3.1 Smoked cigarette butts characteristics

The results for proximate analysis, ultimate analysis, and heating values are frequently used to obtain useful information about the potential use of a feedstock in pyrolytic conversion. After a detailed search in related literature, it was observed that the physicochemical characteristics of the SCB waste are slightly similar to the cashew nutshell, as observed in Table 1. The proximate and ultimate analysis data found in the study performed by Mythili et al. [44] were converted on a dry basis by Eq. 1 and Eq. 2, while the heating values were calculated by Eq. 3 and Eq. 4, to compare with the SCB data. The SCB sample is characterized by higher volatile matter (76.72 wt%) and lower ash content (8.34 wt%) when compared with typical Brazilian coals [45]. This characteristic is attractive for a solid fuel due to a high volatile matter and a low ash content, which are desirable in a feedstock for energy generation. Ash content is critical for biomass conversion since a high ash content can cause undesirable operational issues, such as fouling and slagging, that limit mass and heat transfer [46].

Table 1 Comparative physicochemical characterization between SCB and cashew nutshell

Feedstock	SCB	Cashew nutshell ^c
Proximate analysis (wt%)		
Volatile matter (VM)	76.72 ^a	75.68 ^a
Fixed carbon (FC)	14.94 ^{a,b}	15.83 ^{a,b}
Ash	8.34 ^a	8.49 ^a
VM/FC	5.14	4.78
Ultimate analysis (wt%)		
Carbon (C)	44.46 ^a	46.02 ^a
Hydrogen (H)	6.13 ^a	5.83 ^a
Nitrogen (N)	1.99 ^a	5.44 ^a
Sulfur (S)	< 0.01 ^a	-
Oxygen (O)	39.08 ^{a,b}	34.22 ^{a,b}
Atomic molar ratio		
H/C	1.65	1.52
O/C	0.66	0.56
Heating value		
HHV (MJ kg ⁻¹)	18.50 ^{a,c}	19.14 ^{a,c}
LHV (MJ kg ⁻¹)	17.16 ^{a,d}	17.86 ^{a,d}

^a Dry basis

^b Calculated by difference (Eq. 2)

^c Calculated by Channiwala and Parikh correlation (Eq. 3)

^d Calculated by Eq. 4.

^e Physicochemical characterization from Mythili et al. [44]

The SCB sample contains an amount of fixed carbon content (14.94 wt%) close to those reported for lignocellulosic residues, such as cashew nutshell (15.83 wt%), sugarcane bagasse (14.69 wt%), and sawdust (15.51 wt%) [44]. The solid residue has a high VM/FC ratio (5.14), which is comparable with the typical VM/FC ratios for other biomasses (greater than 4.00). Thus, the SCB can be classified as an adequate energy feedstock in terms of reactivity with easy ignition and a high degree of combustibility [46].

The ultimate analysis showed that the carbon, hydrogen, and oxygen contents were 44.46 wt%, 6.13 wt%, and 39.08 wt%, respectively, for the SCB sample. Typical values of carbon, hydrogen, and oxygen contents found for biowastes are in the following ranges 41.62–48.88 wt%, 5.39–6.22 wt%, and 41.71–46.34 wt%, respectively [44]. Thus, the SCB shows characteristics of a valuable carbonaceous resource for energy recovery or chemical product generation. The SCB sample contains minimal amounts of sulfur (< 0.01 wt%) and nitrogen (1.99 wt%), which minimizes SO_x and NO_x emissions and transform this residue as an environmentally friendly resource for energy. Typical nitrogen amounts found in commercial Brazilian coals are between 0.3 and 1.0 wt% [45]. Despite pyrolysis has been placed as a promising way of disposal for smoked cigarette butts waste, studies

on the combustion behavior and potential emissions also seem interesting goals for future research.

The molar ratios of H/C and O/C for cashew nutshell (1.52 and 0.56, respectively) were lower than the ratios of the SCB sample (1.65 and 0.66, respectively), which is directly correlated to a higher value of HHV for cashew nutshell. The H/C and O/C molar ratios for the SCB sample, as well for cashew nutshell, are comparable with those of lignocellulosic biomasses and vary from 1.52 to 2.05 and from 0.56 to 0.90 for H/C and O/C, respectively [46]. The high HHV of SCB (18.50 MJ kg⁻¹) represents an important advantage of this residue considering its application as an energy feedstock. The HHV value of SCB was superior to that of several lignocellulosic residues such as plum pits (13.71 MJ kg⁻¹), olive pits (17.02 MJ kg⁻¹), sawdust (12.19 MJ kg⁻¹), and jackfruit peel (16.27 MJ kg⁻¹), which are suggested as alternative feedstocks for energy purposes [28, 46].

Slight deviations in physicochemical properties of smoked cigarette butts can occur due to the different cigarette brands and the presence of impurities and humidity in the garbage dump. In addition, it is reported that smoked cigarette butt waste has bulk density ranging from 89.8 to 159.0 kg m⁻³ [47], which is substantially low as compared to the well-established lignocellulosic biomasses for bioenergy, such as coconut shell (293.90 kg m⁻³), sugarcane bagasse (293.00 kg m⁻³), wood sawdust (792.80 kg m⁻³), and rice husk (510.10 kg m⁻³) [44]. The low bulk density of this waste can result in high transportation and handling costs, which can potentially cause a not economically viable processing logistics. In this regard, aiming large-scale processing, low bulk density, and the possible variability in the physicochemical properties of smoked cigarette butt waste can be circumvented by torrefaction combined with densification. The torrefaction is considered a well-established thermochemical pre-treatment to upgrade a low-grade feedstock into a high-grade feedstock with uniform, enhanced physicochemical properties, including reduced moisture content, increased calorific value, and improved energy density [48]. On its turn, the densification processes (such as briquetting) allowed significantly improving the bulk density and energy content per unit volume from different bioenergy feedstocks [49, 50]. Therefore, the use of torrefaction combined with densification can be prospectively explored to make smoked cigarette butts more interesting to be used in waste-to-energy processes.

3.2 Thermal behavior

Figure 1a and Fig. 1b show respectively the TG and DTG profiles obtained for the pyrolysis of smoked cigarette butts under heating rates of 5, 10, 20, and 30 K min⁻¹. The first mass-loss region, at temperatures below 350 K, is attributed to the evaporation of adsorbed moisture. The second and third regions of mass-loss at temperatures between 500 and 700 K

are the active pyrolytic zone, where the maximum devolatilization degree occurs (70.29 ± 2.53 wt% of mass loss). The second mass-loss region can be associated with the decomposition of a small amount of organic volatiles in saturated filters that include tar and nicotine (from 350 to 500 K). The third mass-loss region can be associated with the decomposition of unburned tobacco and cellulose acetate fibers (from 500 to 710 K) [51, 52].

The fitting curve perfectly overlapped with the complex pyrolysis behavior of SCB with a high coefficient of determination ($R^2 = 0.972$) using the Fraser-Suzuki function, as demonstrated at 5 K min⁻¹ (Fig. 1c). This tendency was also verified for all selected heating rates with R^2 close to 1. The active pyrolytic zone can be divided into three pseudo-events: PS-1 (from 350 to 492 K), PS-2 (from 415 to 709 K), and PS-3 (from 559 to 643 K), which correspond to the devolatilization overlapping of the three respective pseudo-components: organic volatiles, unburned tobacco, and cellulose acetate fibers. The application of the Fraser-Suzuki deconvolution function led to the separation of three defined peaks, where the temperature characteristics for the three isolated peaks were slightly shifted to higher values with the increasing heating rate (Fig. 1c). The heat transfer is more effective at higher heating rates than at lower heating rates leading to a devolatilization process at higher temperatures [53]. The isoconversional methods, the compensation effect, and the master plot were applied in the deconvoluted data, where the reaction was considered as three parallel reactions in the active pyrolytic zone to get reliable three kinetic triplets.

3.3 Kinetic triplet examination

3.3.1 Isoconversional estimation of activation energy

The isoconversional methods represented by Eq. 10 (FR method), Eq. 12 (FWO method), Eq. 13 (KAS method), and Eq. 14 (STK method) are solved by a linear relationship; thus, Fig. 2 shows the linear fit over conversion range of $0.1 \leq \alpha \leq 0.9$ for the FR, FWO, KAS, and STK methods for each pseudo-component proposed from deconvolution.

The straight lines with a high coefficient of determination ($R^2 > 0.99$) in Fig. 2 indicate good applicability of all isoconversional methods to determine the values of E_a . In Fig. 2, the parallel straight lines for PS-1 and PS-2 at conversion below 0.2 show a greater gap than those observed for PS-3. This gap is associated with the energy required to breaking the chemical bonds, where the conversion takes place at a lower rate and high-temperature range in the initial conversion. A greater amount of energy is required to solid conversion beginning ($\alpha \leq 0.2$) for PS-1 and PS-2 when compared to PS-3. This behavior can be seen in Fig. 1c; a larger temperature range is required for the initial conversion of PS-1 and PS-2 that results in a flattening of the curve, while the initial

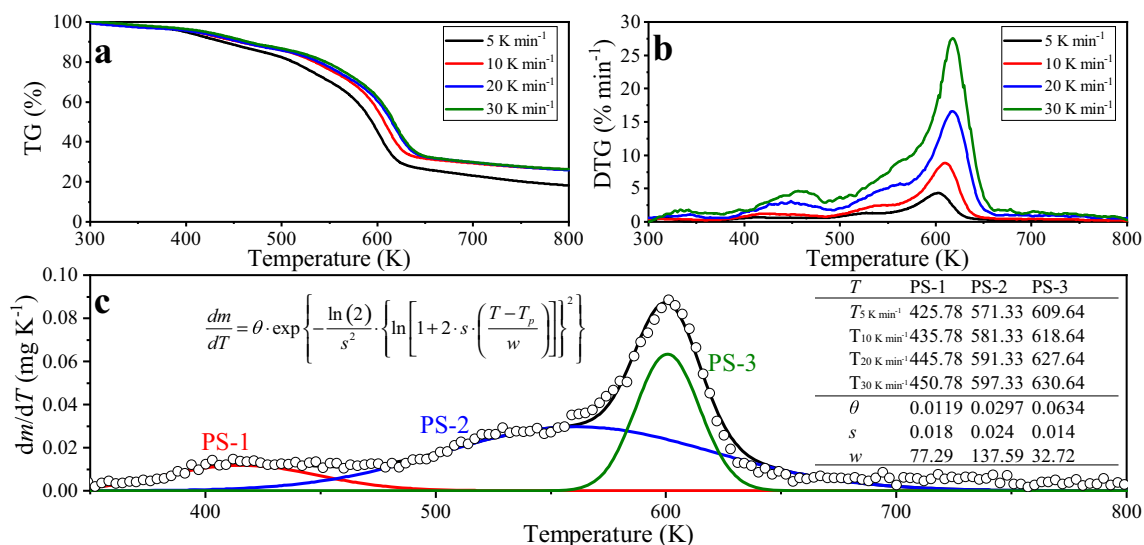


Fig. 1 (a) TG and (b) DTG profiles obtained for the pyrolysis of smoked cigarette butts at 5, 10, 20, and 30 K min⁻¹; and (c) three isolated peaks proposed by the Fraser-Suzuki deconvolution function (at 5 K min⁻¹) and

fitting parameters for each pseudo-component for the pyrolysis of smoked cigarette butts at 5, 10, 20, and 30 K min⁻¹

conversion of PS-3 occurs under a short temperature range. For conversion ranges between 0.2 and 0.8, parallel straight lines are closer than at the beginning of conversion, which has the following order: PS-2 > PS-1 > PS-3. This behavior

indicates that the variation of activation energy as a function of temperature, and conversion, for PS-2 is significantly greater than for PS-3. Thus, there is a relationship between the flattening of the deconvoluted curves (Fig. 1c), where a

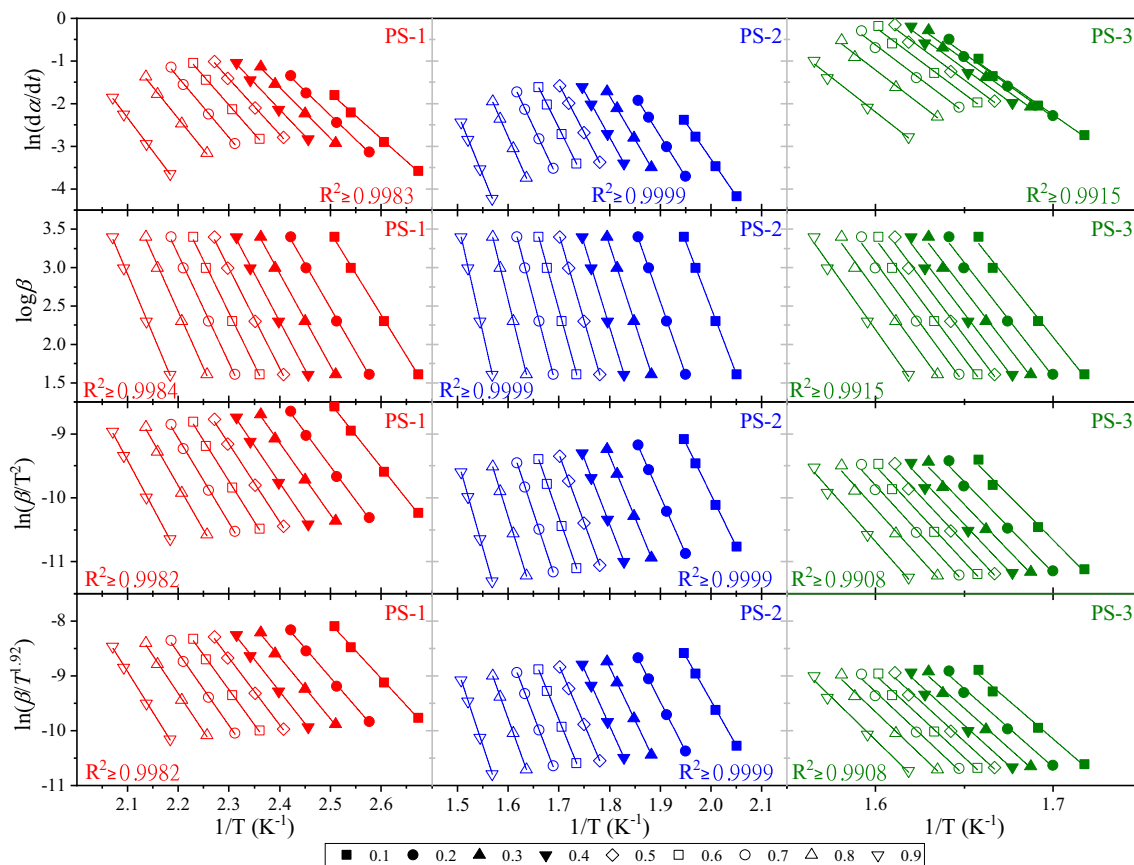


Fig. 2 The linear fit curves obtained from the FR (ln(dα/dt) versus 1/T), FWO (log(β) versus 1/T), KAS (ln(β/T²) versus 1/T), and STK (ln(β/T^{1.92}) versus 1/T) methods for the pseudo-components in SCB pyrolysis

greater temperature range for the complete conversion of a component results in a greater gap between the straight lines; consequently, the variation of activation energy as a function of conversion is associated to the temperature range of deconvoluted curves. A gap is observed at conversion above 0.8 which is similar to conversions below 0.2. In this conversion step, the activation energy increases significantly due to the greater thermal stability of the chemical bonds in the solid structure.

Fig. 3a shows values of E_a obtained for each pseudo-component that was calculated for FR, FWO, KAS, and STK methods at the conversion range of $0.05 \leq \alpha \leq 0.95$. The values of E_a for PS-1 and PS-3 follow a slight increase with conversion ($0.05 \leq \alpha \leq 0.95$), which indicates a slight change in the energy required to the breakdown of the chemical bonds for these pseudo-components. The difference between the observed E_a values for the beginning ($\alpha = 0.05$) and ending ($\alpha = 0.95$) of the thermal decomposition are 50.24–54.26 kJ mol^{-1} and 36.56–38.47 kJ mol^{-1} for PS-1 and PS-3, respectively. The difference of the values of E_a between the beginning ($\alpha = 0.05$) and ending ($\alpha = 0.95$) for PS-2 was 120.81–127.10 kJ mol^{-1} , which is greater than those observed for PS-1 and PS-3. The low E_a values for PS-1 in Fig. 3a indicate that this component can be composed mainly by

semi-volatile (harmful substances such as tar and nicotine), which remain impregnated in the SCB residue after the smoking. This behavior of E_a explains the low temperature at which this component is released (101.87–108.77 kJ mol^{-1}).

For comparison purposes, the activation energy values of other organic materials under pyrolysis conditions are given in Table 2. Kibet et al. [54] evaluated the kinetics of nicotine in mainstream cigarette smoking that was observed to have an E_a value of 108.85 kJ mol^{-1} for a commercial cigarette. The significant increase of E_a values for PS-2 indicates that this component is composed of a complex matrix of compounds. Wang et al. [55] evaluated the E_a values for the pyrolysis of tobacco leaf and was observed an average value of 131.74 kJ mol^{-1} . Zhao et al. [56] studied the effect of inorganic and organic salts on the pyrolysis of cigarette paper, in which a decrease of E_a values was observed when inorganic and organic salts were added (225.4–251.8 kJ mol^{-1} to 134.2–203.4 kJ mol^{-1}). Based on these data, it can be assumed that the values of E_a for PS-2 represent the complex and majority decomposition of unburned tobacco, carbonized tobacco, and paper. The values of E_a for PS-3 can be associated with the energy required for cellulose acetate decomposition, where similar E_a values were observed by Henrique et al. [57] during

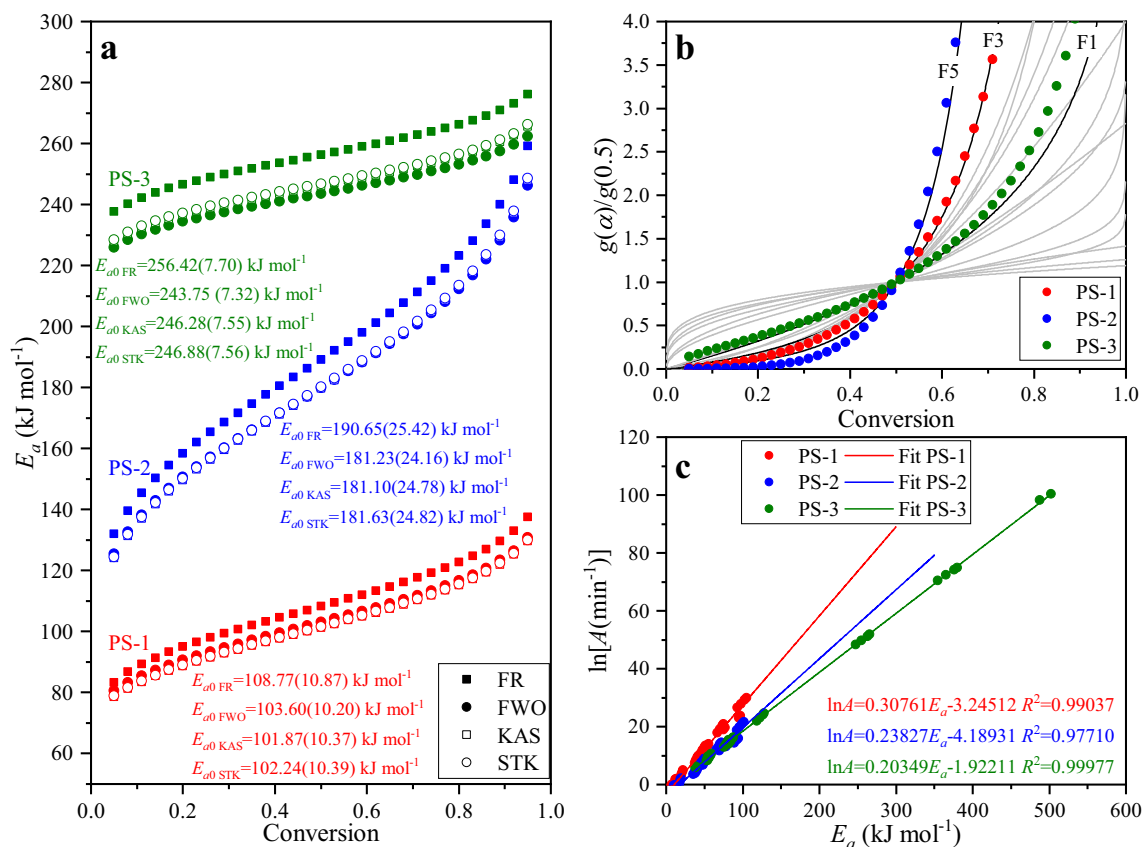


Fig. 3 (a) E_a versus α curves obtained from FR, FWO, KAS, and STK, (b) master plot curves between (symbol) experimental and (line) theoretical data, and (c) linear fitted obtained from compensation effect for PS-1, PS2, and PS-3

Table 2 Comparison of apparent activation energy for the pyrolysis of smoked cigarette butts with literature values for other organic materials under pyrolysis conditions

Reference	Feedstock	Heating rate (K min ⁻¹)	Kinetic method	E_a (kJ mol ⁻¹)
This study	SCB	5, 10, 20, and 30	Multi-step kinetics (Starink)	102.24 for PS-1 181.63 for PS-2 246.88 for PS-3
Ref. [40]	Sub-bituminous coal	5, 10, and 20	Single-step kinetics (FWO)	287.40 (average)
Ref. [54]	Nicotine	--	--	108.85
Ref. [55]	Tobacco leaf	5, 10, and 15	Single-step kinetics (DAEM)	131.74
Ref. [56]	Cigarette paper	20	Single-step kinetics (Coats–Redfern)	251.80
Ref. [57]	Cellulose nanocrystals	5, 10, 20, and 40	Single-step kinetics (FWO)	241.24 (average)

the thermal decomposition of cellulose nanocrystals. In general, the values of E_a were lower than those obtained for sub-bituminous coal (277.3–287.4 kJ mol⁻¹) [40], which can indicate suitable applicability in the pyrolysis process. A lower activation energy is often associated with a fast reaction and high reactivity [18].

3.3.2 Reaction model determination

The reaction model ($f(\alpha)$) estimated by the master plot method appears as n th-order reaction mechanisms of the considered pseudo-components, as shown in Fig. 3b (F3 for PS-1, F5 for PS-2, and F1 for PS-3). It is observed that the pyrolysis of smoked cigarette butts occur from several parallel n th-order reactions, where the devolatilization starts with a third-order reaction ($f(\alpha)_{\text{PS-1}} = (1-\alpha)^3$), followed by a fifth-order reaction ($f(\alpha)_{\text{PS-2}} = (1-\alpha)^5$), and ending as first-order reaction ($f(\alpha)_{\text{PS-3}} = 1-\alpha$). Higher order reaction observed for PS-1 and PS-2 can be explained by the blocking of surface pores by low-temperature decomposition products of smoked cigarette butts, causing the hindrance of volatile releases [40]. The presence of several parallel n th-order reactions also was reported for the pyrolysis of plastic solid waste [1].

3.3.3 Frequency factor estimation

Satisfactory values of R^2 were obtained from the compensation effect for PS-1 ($R^2 = 0.9904$), PS-2 ($R^2 = 0.9771$), and PS-3 ($R^2 = 0.9998$), which provided values of frequency factor (A) of $1.77 \times 10^{12} \text{ min}^{-1}$ ($\ln A_{\text{PS-1}} = 28.20$) for PS-1, $9.44 \times 10^{16} \text{ min}^{-1}$ ($\ln A_{\text{PS-2}} = 39.09$) for PS-2, and $9.62 \times 10^{20} \text{ min}^{-1}$ ($\ln A_{\text{PS-3}} = 48.32$) for PS-3 (Fig. 3c). These different values of A can be attributed to the different composition of the pseudo-components. High values of the frequency factor imply in an easier decomposition [18], where values of A for PS-3 ($\sim 10^{20} \text{ min}^{-1}$) appeared to be quicker and easier to start devolatilization than PS-1 and PS-2 ($\sim 10^{12}$ – 10^{16} min^{-1}). The frequency factor with magnitude lower than 10^9 indicates

a surface reaction, while the frequency factor with an order of magnitude higher or equal to 10^9 indicates simpler reaction chemistry [17]. The values of E_a higher than 100 kJ mol^{-1} and A with a magnitude higher than 10^{12} min^{-1} imply that the pyrolysis of smoked cigarette butts is chemically controlled [16].

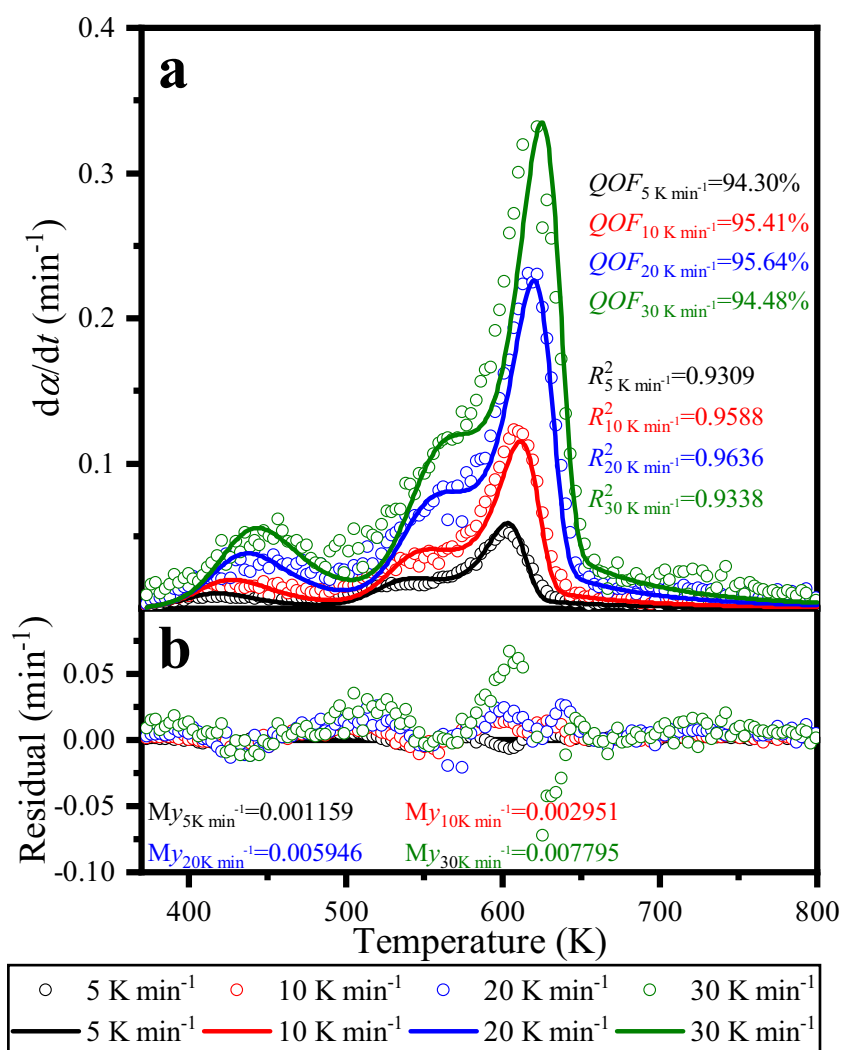
3.3.4 Simulated

The kinetic triplet estimated can be applied in Eq. 6 to provide an expression that represents the thermal decomposition of SCB. The contributed fractions for PS-1, PS-2, and PS-3 were 0.1445, 0.3865, and 0.3268, respectively. When compared to the isoconversional methods of FR, FWO, and KAS, the STK method improves the accuracy of the activation energy satisfactorily [23, 34, 58]. That is the reason why the activation energies obtained with the STK method were used into the overall kinetic expression (Eq. 25) and also to derive the thermodynamic parameters.

$$\left(\frac{d\alpha}{dt}\right) = 0.1445 \cdot (1.77 \times 10^{12}) \cdot e^{-102240/RT} \cdot (1-\alpha)^3 + 0.3865 \cdot (9.44 \times 10^{16}) \cdot e^{-181630/RT} \cdot (1-\alpha)^5 + 0.3268 \cdot (9.62 \times 10^{20}) \cdot e^{-246880/RT} \cdot (1-\alpha) \quad (25)$$

Figure 4a shows a satisfactory equivalence between the experimental and reconstructed curves, which obtained high values of the coefficient of determination ($R^2 > 0.93$). The coefficient of determination indicates that the set of kinetic triplets obtained from deconvolution can describe adequately the decomposition process of SCB. The value of QOF was above 94.30% and shows a deviation between the experimental and reconstructed curves of less than 5.70%. These values of QOF are acceptable since most of the thermal behavior could be described. Based on this information, Eq. 25 can describe acceptably the thermal behavior of the SCB under an oxygen-free atmosphere. On the other hand, some

Fig. 4 (a) Reconstructed (line) and experimental (symbol) curves of $d\alpha/dt$ versus T for pyrolysis of SCB at heating rate of 5, 10, 20, and 30 K min⁻¹ and (b) respective residuals



temperature regions were described with a low adjustment, as seen in Fig. 4b. The low adjustment was observed in some temperature regions for the heating rate of 30 K min⁻¹. These regions comprise the temperature range between the end of PS-1 decomposition and the beginning of PS-2 decomposition (483–530 K), and some experimental points at a high decomposition rate. The high relative error at high decomposition rate can be associated with some noise in experimental data; experimental data can influence the high deviations between the calculated data, which leads to the difference of these values. This slight deviation can also be explained by a significant delay in the heat transfer, which is usually reported for the pyrolysis of solid waste under high decomposition rates [22]. On the other hand, the average value of the residual for the heating rate of 30 K min⁻¹ was 0.00795, which represents a low value when compared to the regions with the high values of relative error. In general, it is noted that the data of kinetic triplet can describe the pyrolysis process of the SCB and the data can assist in the optimization and modeling of a pyrolysis reactor for this type of waste.

3.4 Thermodynamic analysis

The thermodynamic parameters (ΔH , ΔG , and ΔS) calculated for the three pseudo-components by using the E_a values are shown in Table 3. Average values of ΔH were calculated as 98.67 kJ mol⁻¹, 176.84 kJ mol⁻¹, and 241.79 kJ mol⁻¹ for PS-1, PS-2, and PS-3, respectively.

The positive values of ΔH indicate an endothermic aspect of the pyrolysis of smoked cigarette butts, which confirm the requirement of an external energy source to produce biofuels under an oxygen-free atmosphere. Furthermore, the E_a - ΔH values were lower than 5.09 kJ mol⁻¹ that indicates a facility to overcome the potential energy barrier, which is related to an energy-efficient manner to product formation [1, 17].

Changes of the Gibbs free energy (ΔG) were estimated to be 122.63 kJ mol⁻¹ for PS-1, 158.29 kJ mol⁻¹ for PS-2, and 175.43 kJ mol⁻¹ for PS-3. The ΔH and ΔG values were positive, and suggest a non-spontaneous decomposition reaction that needs heat to occur [16]. The high value of ΔG

Table 3 Thermodynamic parameter calculated for the pseudo-components (PS-1, PS-2, and PS-3) of SCB

Conversion	PS-1			PS-2			PS-3		
	ΔH (kJ mol ⁻¹)	ΔG (kJ mol ⁻¹)	ΔS (J mol ⁻¹ K ⁻¹)	ΔH (kJ mol ⁻¹)	ΔG (kJ mol ⁻¹)	ΔS (J mol ⁻¹ K ⁻¹)	ΔH (kJ mol ⁻¹)	ΔG (kJ mol ⁻¹)	ΔS (J mol ⁻¹ K ⁻¹)
0.05	99.11	119.68	-54.70	177.63	161.41	33.73	241.98	177.89	108.78
0.1	99.09	119.83	-54.76	177.58	161.24	33.64	241.97	177.76	108.76
0.15	99.07	119.97	-54.82	177.55	161.09	33.56	241.96	177.64	108.75
0.2	99.05	120.10	-54.87	177.51	160.95	33.49	241.95	177.54	108.73
0.25	99.03	120.21	-54.91	177.48	160.83	33.43	241.95	177.44	108.72
0.3	99.02	120.31	-54.95	177.46	160.72	33.38	241.94	177.35	108.71
0.35	99.00	120.41	-54.99	177.43	160.61	33.32	241.93	177.27	108.70
0.4	98.99	120.50	-55.02	177.40	160.51	33.28	241.93	177.20	108.69
0.45	98.98	120.59	-55.06	177.38	160.42	33.23	241.92	177.12	108.68
0.5	98.96	120.67	-55.09	177.36	160.33	33.19	241.92	177.06	108.67
0.55	98.95	120.74	-55.12	177.34	160.25	33.15	241.91	176.99	108.66
0.6	98.94	120.82	-55.15	177.32	160.17	33.11	241.91	176.93	108.65
0.65	98.93	120.89	-55.17	177.30	160.09	33.07	241.90	176.87	108.65
0.7	98.92	120.96	-55.20	177.28	160.02	33.04	241.90	176.81	108.64
0.75	98.91	121.03	-55.23	177.26	159.95	33.00	241.89	176.75	108.63
0.8	98.90	121.09	-55.25	177.25	159.88	32.97	241.89	176.70	108.62
0.85	98.89	121.15	-55.27	177.23	159.81	32.94	241.88	176.65	108.62
0.9	98.88	121.22	-55.30	177.21	159.75	32.91	241.88	176.59	108.61
0.95	98.22	125.69	-56.80	176.03	155.21	30.93	241.60	172.93	108.16
Average ^a	98.67 (0.18)	122.63 (1.21)	-55.79 (0.42)	176.84 (0.32)	158.29 (1.24)	32.25 (0.56)	241.79 (0.08)	175.43 (0.99)	108.46 (0.12)

^a Calculated for all conversion data (variation of 0.001)

denotes a lower favorability for pyrolytic conversion [18]. The ΔG values found during the pyrolysis of smoked cigarette butts (from 122.63 to 175.43 kJ mol⁻¹) are in agreement with the range found for pyrolysis of plastic solid waste (from 160.96 to 215.56 kJ mol⁻¹) [1], PVC cable sheath (from 158.95 to 162.19 kJ mol⁻¹) [17], medium density fiberboard (from 147.87 to 169.20 kJ mol⁻¹) [18], and coffee paper cup waste (from 138.50 to 141.90 kJ mol⁻¹) [16]. This insight indicated that the conversion of smoked cigarette butts to energy is comparable with the abovementioned typical solid wastes in terms of favorability.

It is well known that the values of ΔS manifest the degree of disorder of a pyrolysis reaction. The negative value of ΔS for PS-1 (-55.79 J mol⁻¹ K⁻¹) indicates that the first devolatilization event has a lower reactive characteristic associated with a higher degree of arrangement [16, 28]. This insight can be interpreted as a thermally stable product that has been produced, i.e., the activated complex produced presents a more well-organized structure than that in the initial state [1, 17]. This indicates that the decomposition of the complex matrix of compounds in SCB is close to its thermodynamic equilibrium. The

ΔS values for PS-2 (32.25 J mol⁻¹ K⁻¹) and PS-3 (108.46 J mol⁻¹ K⁻¹) were positive, which is associated with a higher reactive characteristic, indicating that less time is required for the activated complex generation [1]. Thus, in terms of the activated complex theory [41–43], the pyrolysis of smoked cigarette butts can be described as an initial “slow” devolatilization event for PS-1 (tar and nicotine), followed by “fast” devolatilization events for PS-2 (unburned tobacco) and PS-3 (cellulose acetate fibers). The negative and positive ΔS values during the pyrolysis of smoked cigarette butts can be interpreted as a result of the complex reactions involved. This tendency is consistent with other kinds of solid waste proposed as feedstocks for pyrolysis, such as PVC cable sheath and plastic solid waste [1, 17]. The thermodynamic analysis suggests the smoked cigarette butts as a suitable feedstock for pyrolysis with excellent prospects to produce energy, illustrating the opportunity of making good use of this solid residue with toxic characteristics. Future research directions will include investigating the pyrolysis of smoked cigarette butts on a bench-scale reactor to gain insight into the product yields and their characterization.

4 Conclusions

For the first time, it is revealed how smoked cigarette butt waste may be a suitable energy feedstock under pyrolysis kinetics and thermodynamics aspects. This paper addressed the pyrolysis of smoked cigarette butts in the form of multiple-step kinetics, with the contribution of three pseudo-components distinguished and quantified using deconvolution with the asymmetrical Fraser-Suzuki function. The order of magnitude of the frequency factor indicates a simpler reaction pathway for the decomposition of smoked cigarette butts. All pseudo-components obey n th-order reaction mechanisms according to the master plot method. The kinetic triplets were satisfactorily able to reconstruct original experimental curves. It is worth highlighting that the deconvolution combined with isoconversional analysis used here can potentially be extended to other solid wastes with multiple-step kinetic behaviors. Findings related to thermodynamic investigations attested to the endothermic and non-spontaneous nature of the pyrolysis of smoked cigarette butts. The value of $E_a - \Delta H$ smaller than 5.09 kJ mol^{-1} implies that pyrolysis is potentially able to convert smoked cigarette butts in energy in a viable manner. The reported results confirm that smoked cigarette butts are a suitable feedstock toward renewable energy production.

Funding This work was supported by Brazil's National Council for Scientific and Technological Development (CNPq/Brazil Process 423869/2016-7) and Brazil's Coordination for the Improvement of Higher Education Personnel (CAPES/Brazil Finance Code 001). This work was developed in the Laboratory of Activated Carbon (LCA/UFPB) and Laboratory of Control and Polymerization Processes (LCP/UFSC).

Nomenclature and Symbolology A (min^{-1}), frequency factor; a (dimensionless), compensation parameter; b (dimensionless), compensation parameter; c (dimensionless), contributed fraction in conversion; DTG (wt\% min^{-1}), differential thermogravimetric; $(d\alpha/dt)_{av}$ (min^{-1}), average of experimental values; $(d\alpha/dt)_{dec}$ (min^{-1}), values from deconvolution; $(d\alpha/dt)_{exp}$ (min^{-1}), experimental values measured; E_a (kJ mol^{-1}), apparent activation energy; $f(\alpha)$ (dimensionless), reaction model; FC (wt%), fixed carbon; FR, Friedman; FWO, Flynn-Wall-Ozawa; $g(\alpha)$ (dimensionless), integral form of the reaction model; HHV (MJ kg^{-1}), higher heating value; h (J s^{-1}), Plank constant; KAS, Kissinger-Akahira-Sunose; k_B (J K^{-1}), Boltzmann constant; LHV (MJ kg^{-1}), lower heating value; M (dimensionless), total number of points used for deconvolution; M_y (dimensionless), mean residual; m_0 (g), initial mass; m_∞ (g), final mass; N (dimensionless), total of components proposed for residue; $p(x)$ (dimensionless), approximation for temperature integral equation; PS, pseudo-component; QOF (dimensionless), quality of fit; R ($\text{kJ mol}^{-1} \text{K}^{-1}$), gas constant; R^2 (dimensionless), coefficient of determination; RSS (dimensionless), residual sum of squares; s (dimensionless), asymmetry shape parameter; SCB, smoked cigarette butts; STK, Starink; t (min), time; T (K), temperature; TGA (wt%), thermogravimetric analysis; T_m (K), maximum temperature peak; T_p (K), peak temperature; VM (wt%), volatile matter; w (dimensionless), half-width in the curve; y (dimensionless), residual; α (dimensionless), physical parameters of conversion; β (K min^{-1}), heating rate; η (dimensionless), contribution of pseudo-component; θ

(dimensionless), amplitude; ΔG (kJ mol^{-1}), Gibb's free energy change; ΔH (kJ mol^{-1}), enthalpy change; ΔS ($\text{J mol}^{-1} \text{K}^{-1}$), entropy change

References

- Mumbach GD, Alves JLF, Da Silva JCG et al (2019) Thermal investigation of plastic solid waste pyrolysis via the deconvolution technique using the asymmetric double sigmoidal function: determination of the kinetic triplet, thermodynamic parameters, thermal lifetime and pyrolytic oil composition for clean. *Energy Convers Manag* 200:112031. <https://doi.org/10.1016/j.enconman.2019.112031>
- Czajczyńska D, Anguilano L, Ghazal H, Krzyżyńska R, Reynolds AJ, Spencer N, Jouhara H (2017) Potential of pyrolysis processes in the waste management sector. *Therm Sci Eng Prog* 3:171–197. <https://doi.org/10.1016/j.tsep.2017.06.003>
- Glugoski LP, de Jesus CP, Fujiwara ST (2017) Reactive Black 5 dye degradation using filters of smuggled cigarette modified with Fe3+. *Environ Sci Pollut Res* 24:6143–6150. <https://doi.org/10.1007/s11356-016-6820-0>
- d'Henri Teixeira MB, Duarte MAB, Raposo Garcez L, Camargo Rubim J, Hofmann Gatti T, Suarez PAZ (2017) Process development for cigarette butts recycling into cellulose pulp. *Waste Manag* 60:140–150. <https://doi.org/10.1016/j.wasman.2016.10.013>
- Sun H, La P, Yang R et al (2017) Innovative nanoporous carbons with ultrahigh uptakes for capture and reversible storage of CO2 and volatile iodine. *J Hazard Mater* 321:210–217. <https://doi.org/10.1016/j.jhazmat.2016.09.015>
- Slaughter E, Gersberg RM, Watanabe K, Rudolph J, Stransky C, Novotny TE (2011) Toxicity of cigarette butts, and their chemical components, to marine and freshwater fish. *Tob Control* 20:i25–i29. <https://doi.org/10.1136/tc.2010.040170>
- Soltani SM, Yazdi SK, Hosseini S, Gargari MK (2014) Effect of nitric acid modification on porous characteristics of mesoporous char synthesized from the pyrolysis of used cigarette filters. *J Environ Chem Eng* 2:1301–1308. <https://doi.org/10.1016/j.jece.2014.04.005>
- Wang W, Wang M, Huang J, Li X, Cai L, Shi SQ, Cui Y, Chen L, Ni Y (2020) High efficiency pyrolysis of used cigarette filters for ester-rich bio-oil through microwave-assisted heating. *J Clean Prod* 257:120596. <https://doi.org/10.1016/j.jclepro.2020.120596>
- Koochaki CB, Khajavi R, Rashidi A, Mansouri N, Yazdanshenas ME (2019) The effect of pre-swelling on the characteristics of obtained activated carbon from cigarette butts fibers. *Biomass Convers Biorefinery* 10:227–236. <https://doi.org/10.1007/s13399-019-00429-x>
- Naqvi SR, Prabhakara HM, Bramer EA, Dierkes W, Akkerman R, Brem G (2018) A critical review on recycling of end-of-life carbon fibre/glass fibre reinforced composites waste using pyrolysis towards a circular economy. *Resour Conserv Recycl* 136:118–129. <https://doi.org/10.1016/j.resconrec.2018.04.013>
- Qureshi MS, Oasmaa A, Pihkola H, Deviatkin I, Tenhunen A, Mannila J, Minkkinen H, Pohjakallio M, Laine-Ylijoki J (2020) Pyrolysis of plastic waste: opportunities and challenges. *J Anal Appl Pyrolysis* 148:104804. <https://doi.org/10.1016/j.jaap.2020.104804>
- Naqvi SR, Uemura Y, Osman NB, Yusup S, Nuruddin MF (2014) Physicochemical properties of pyrolysis oil derived from fast pyrolysis of wet and dried rice husk in a free fall reactor. *Appl Mech Mater* 625:604–607. <https://doi.org/10.4028/www.scientific.net/AMM.625.604>
- Samolada MC, Zabaniotou AA (2014) Comparative assessment of municipal sewage sludge incineration, gasification and pyrolysis for a sustainable sludge-to-energy management in Greece. *Waste*

- Manag 34:411–420. <https://doi.org/10.1016/j.wasman.2013.11.003>
14. Beneroso D, Bermúdez JM, Arenillas A, Menéndez JA (2014) Influence of the microwave absorbent and moisture content on the microwave pyrolysis of an organic municipal solid waste. *J Anal Appl Pyrolysis* 105:234–240. <https://doi.org/10.1016/j.jaap.2013.11.009>
 15. Borges NB, Campos JR, Pablos JM (2015) Characterization of residual sand removed from the grit chambers of a wastewater treatment plant and its use as fine aggregate in the preparation of non-structural concrete. *Water Pract Technol* 10:164–171. <https://doi.org/10.2166/wpt.2015.018>
 16. Janković B (2014) The pyrolysis of coffee paper cup waste samples using non-isothermal thermo-analytical techniques. The use of combined kinetic and statistical analysis in the interpretation of mechanistic features of the process. *Energy Convers Manag* 85: 33–49. <https://doi.org/10.1016/j.enconman.2014.05.094>
 17. Liu H, Wang C, Zhang J, Zhao W, Fan M (2020) Pyrolysis kinetics and thermodynamics of typical plastic waste. *Energy Fuel* 34: 2385–2390. <https://doi.org/10.1021/acs.energyfuels.9b04152>
 18. Aslan DI, Özoğul B, Ceylan S, Geyikçi F (2018) Thermokinetic analysis and product characterization of medium density fiberboard pyrolysis. *Bioresour Technol* 258:105–110. <https://doi.org/10.1016/j.biortech.2018.02.126>
 19. Tahir MH, Çakman G, Goldfarb JL, Topcu Y, Naqvi SR, Ceylan S (2019) Demonstrating the suitability of canola residue biomass to biofuel conversion via pyrolysis through reaction kinetics, thermodynamics and evolved gas analyses. *Bioresour Technol* 279:67–73. <https://doi.org/10.1016/j.biortech.2019.01.106>
 20. White JE, Catallo WJ, Legendre BL (2011) Biomass pyrolysis kinetics: a comparative critical review with relevant agricultural residue case studies. *J Anal Appl Pyrolysis* 91:1–33. <https://doi.org/10.1016/j.jaap.2011.01.004>
 21. Yao Z, Yu S, Su W, Wu W, Tang J, Qi W (2020) Kinetic studies on the pyrolysis of plastic waste using a combination of model-fitting and model-free methods. *Waste Manag Res* 38:77–85. <https://doi.org/10.1177/0734242X19897814>
 22. Mishra A, Kumari U, Turlapati VY, Siddiqi H, Meikap BC (2020) Extensive thermogravimetric and thermo-kinetic study of waste motor oil based on iso-conversional methods. *Energy Convers Manag* 221:113194. <https://doi.org/10.1016/j.enconman.2020.113194>
 23. da Silva JCG, de Albuquerque JG, Galdino WV de A, et al. (2020) Single-step and multi-step thermokinetic study – deconvolution method as a simple pathway for describe properly the biomass pyrolysis for energy conversion. *Energy Convers Manag* 209: 112653. <https://doi.org/10.1016/j.enconman.2020.112653>
 24. Siddiqi H, Kumari U, Biswas S, Mishra A, Meikap BC (2020) A synergistic study of reaction kinetics and heat transfer with multi-component modelling approach for the pyrolysis of biomass waste. *Energy* 204:117933. <https://doi.org/10.1016/j.energy.2020.117933>
 25. Hameed Z, Naqvi SR, Naqvi M, Ali I, Taqvi SAA, Gao N, Hussain SA, Hussain S (2020) A comprehensive review on thermal coconversion of biomass, sludge, coal, and their blends using thermogravimetric analysis. *J Chemother* 2020:1–23. <https://doi.org/10.1155/2020/5024369>
 26. Naqvi SR, Ali I, Nasir S, Ali Ammar Taqvi S, Atabani AE, Chen WH (2020) Assessment of agro-industrial residues for bioenergy potential by investigating thermo-kinetic behavior in a slow pyrolysis process. *Fuel* 278:118259. <https://doi.org/10.1016/j.fuel.2020.118259>
 27. Hameed Z, Aman Z, Naqvi SR, Tariq R, Ali I, Makki AA (2018) Kinetic and thermodynamic analyses of sugar cane bagasse and sewage sludge co-pyrolysis process. *Energy Fuel* 32:9551–9558. <https://doi.org/10.1021/acs.energyfuels.8b01972>
 28. Fernandez A, Ortiz LR, Asensio D, Rodriguez R, Mazza G (2020) Kinetic analysis and thermodynamics properties of air/steam gasification of agricultural waste. *J Environ Chem Eng* 8:103829. <https://doi.org/10.1016/j.jece.2020.103829>
 29. Vyazovkin S, Burnham AK, Criado JM, Pérez-Maqueda LA, Popescu C, Sbirrazzuoli N (2011) ICTAC Kinetics Committee recommendations for performing kinetic computations on thermal analysis data. *Thermochim Acta* 520:1–19. <https://doi.org/10.1016/j.tca.2011.03.034>
 30. Manić N, Janković B, Pijović M, Waisi H, Dodevski V, Stojiljković D, Jovanović V (2020) Apricot kernel shells pyrolysis controlled by non-isothermal simultaneous thermal analysis (STA). *J Therm Anal Calorim*. <https://doi.org/10.1007/s10973-020-09307-5>
 31. ASTM (2014) E1131-08: Standard test method for compositional analysis by thermogravimetry. In: Annual Book of ASTM Standards. ASTM International, West Conshohocken, pp 1– 6. <https://doi.org/10.1520/E1131-08R14>
 32. ASTM (2008) D5373-08: Standard test methods for instrumental determination of carbon, hydrogen, and nitrogen in laboratory samples of coal. In: Annual Book of ASTM Standards. ASTM International, West Conshohocken, pp 1–9. <https://doi.org/10.1520/D5373-08>
 33. Channiwala SA, Parikh PP (2002) A unified correlation for estimating HHV of solid, liquid and gaseous fuels. *Fuel* 81:1051–1063. [https://doi.org/10.1016/S0016-2361\(01\)00131-4](https://doi.org/10.1016/S0016-2361(01)00131-4)
 34. Alves JLF, Da Silva JCG, da Silva Filho VF et al (2019) Bioenergy potential of red macroalgae *Gelidium floridanum* by pyrolysis: evaluation of kinetic triplet and thermodynamics parameters. *Bioresour Technol* 291:121892. <https://doi.org/10.1016/j.biortech.2019.121892>
 35. Van de Velden M, Baeyens J, Boukis I (2008) Modeling CFB biomass pyrolysis reactors. *Biomass Bioenergy* 32:128–139. <https://doi.org/10.1016/j.biombioe.2007.08.001>
 36. Vyazovkin S, Chrissafis K, Di Lorenzo ML et al (2014) ICTAC Kinetics Committee recommendations for collecting experimental thermal analysis data for kinetic computations. *Thermochim Acta* 590:1–23. <https://doi.org/10.1016/j.tca.2014.05.036>
 37. Alves JLF, Da Silva JCG, da Silva Filho VF et al (2019) Determination of the bioenergy potential of Brazilian pine-fruit shell via pyrolysis kinetics, thermodynamic study, and evolved gas analysis. *Bioenergy Res* 12:168–183. <https://doi.org/10.1007/s12155-019-9964-1>
 38. Perejón A, Sánchez-Jiménez PE, Criado JM, Pérez-Maqueda LA (2011) Kinetic analysis of complex solid-state reactions. A new deconvolution procedure. *J Phys Chem B* 115:1780–1791. <https://doi.org/10.1021/jp110895z>
 39. Vyazovkin S (2015) Isoconversional kinetics of thermally stimulated processes, 1st edn. Springer International Publishing, Cham
 40. Konwar K, Nath HP, Bhuyan N, Saikia BK, Borah RC, Kalita AC, Saikia N (2019) Effect of biomass addition on the devolatilization kinetics, mechanisms and thermodynamics of a northeast Indian low rank sub-bituminous coal. *Fuel* 256:115926. <https://doi.org/10.1016/j.fuel.2019.115926>
 41. Boonchom B (2008) Kinetics and thermodynamic properties of the thermal decomposition of manganese dihydrogenphosphate dihydrate. *J Chem Eng Data* 53:1533–1538. <https://doi.org/10.1021/je800103w>
 42. Danvirutai C, Noisong P, Youngme S (2010) Some thermodynamic functions and kinetics of thermal decomposition of $\text{NH}_4\text{MnPO}_4 \cdot \text{H}_2\text{O}$ in nitrogen atmosphere. *J Therm Anal Calorim* 100:117–124. <https://doi.org/10.1007/s10973-009-0017-4>
 43. Boonchom B, Puttawong S (2010) Thermodynamics and kinetics of the dehydration reaction of $\text{FePO}_4 \cdot 2\text{H}_2\text{O}$. *Phys B Condens Matter* 405:2350–2355. <https://doi.org/10.1016/j.physb.2010.02.046>

44. Mythili R, Venkatachalam P, Subramanian P, Uma D (2013) Characterization of bioresidues for biooil production through pyrolysis. *Bioresour Technol* 138:71–78. <https://doi.org/10.1016/j.biortech.2013.03.161>
45. Kalkreuth W, Holz M, Kern M, Machado G, Mexias A, Silva MB, Willett J, Finkelman R, Burger H (2006) Petrology and chemistry of Permian coals from the Paraná Basin: 1. Santa Terezinha, Leão-Butiá and Candiota Coalfields, Rio Grande do Sul, Brazil. *Int J Coal Geol* 68:79–116. <https://doi.org/10.1016/j.coal.2005.10.006>
46. Alves JLF, da Silva JCG, Mumbach GD, Domenico MD, da Silva Filho VF, de Sena RF, Machado RAF, Marangoni C (2020) Insights into the bioenergy potential of jackfruit wastes considering their physicochemical properties, bioenergy indicators, combustion behaviors, and emission characteristics. *Renew Energy* 155:1328–1338. <https://doi.org/10.1016/j.renene.2020.04.025>
47. Maderuelo-Sanz R, Gómez Escobar V, Meneses-Rodríguez JM (2018) Potential use of cigarette filters as sound porous absorber. *Appl Acoust* 129:86–91. <https://doi.org/10.1016/j.apacoust.2017.07.011>
48. Olugbade TO, Ojo OT (2020) Biomass Torrefaction for the production of high-grade solid biofuels: a review. *BioEnergy Res*. <https://doi.org/10.1007/s12155-020-10138-3>
49. Olugbade T, Ojo O, Mohammed T (2019) Influence of binders on combustion properties of biomass briquettes: a recent review. *BioEnergy Res* 12:241–259. <https://doi.org/10.1007/s12155-019-09973-w>
50. Olugbade TO, Ojo OT (2020) Binderless briquetting technology for lignite briquettes: a review. *Energy, Ecol Environ*. <https://doi.org/10.1007/s40974-020-00165-3>
51. Fan G, Liao C, Fang T, Luo S, Song G (2014) Amberlyst 15 as a new and reusable catalyst for the conversion of cellulose into cellulose acetate. *Carbohydr Polym* 112:203–209. <https://doi.org/10.1016/j.carbpol.2014.05.082>
52. Calabuig E, Juárez-Serrano N, Marcilla A (2019) TG-FTIR study of evolved gas in the decomposition of different types of tobacco. Effect of the addition of SBA-15. *Thermochim Acta* 671:209–219. <https://doi.org/10.1016/j.tca.2018.12.006>
53. Idris SS, Rahman NA, Ismail K (2012) Combustion characteristics of Malaysian oil palm biomass, sub-bituminous coal and their respective blends via thermogravimetric analysis (TGA). *Bioresour Technol* 123:581–591. <https://doi.org/10.1016/j.biortech.2012.07.065>
54. Kibet J, Kurgat C, Limo S, Rono N, Bosire J (2016) Kinetic modeling of nicotine in mainstream cigarette smoking. *Chem Cent J* 10:60. <https://doi.org/10.1186/s13065-016-0206-8>
55. Wang X, Wang Z, Dai Y, Ma K, Zhu L, Tan H (2017) Thermogravimetric study on the flue-cured tobacco leaf pyrolysis and combustion using a distributed activation energy model. *Asia-Pacific J Chem Eng* 12:75–84. <https://doi.org/10.1002/apj.2055>
56. Zhao D, Dai Y, Chen K, Sun Y, Yang F, Chen K (2013) Effect of potassium inorganic and organic salts on the pyrolysis kinetics of cigarette paper. *J Anal Appl Pyrolysis* 102:114–123. <https://doi.org/10.1016/j.jaap.2013.03.007>
57. Henrique MA, Flauzino Neto WP, Silvério HA, Martins DF, Gurgel LVA, Barud HS, Morais LC, Pasquini D (2015) Kinetic study of the thermal decomposition of cellulose nanocrystals with different polymorphs, cellulose I and II, extracted from different sources and using different types of acids. *Ind Crop Prod* 76:128–140. <https://doi.org/10.1016/j.indcrop.2015.06.048>
58. Starink MJ (2003) The determination of activation energy from linear heating rate experiments: A comparison of the accuracy of isoconversion methods. *Thermochim Acta* 404:163–176. [https://doi.org/10.1016/S0040-6031\(03\)00144-8](https://doi.org/10.1016/S0040-6031(03)00144-8)

Publisher's Note Springer Nature remains neutral with regard to jurisdictional claims in published maps and institutional affiliations.